Science and Technology Publishing (SCI & TECH)
ISSN: 2632-1017
Vol. 6 Issue 5, May - 2022

Design Of Satellite Orbital Two Line Element To Cartesian Position Vector Coordinates Transformation Program

Okon, Abasiama Colman[1]
Department of Computer Engineering
Akwa Ibom State Polytechnic , Ikot Osurua Ikot Ekpene

Ufot Okon Nsa[2]
Department of Computer Engineering
Akwa Ibom State Polytechnic , Ikot Osurua Ikot Ekpene

Uduak Etim Udoka[3]
Department of Computer Engineering
Akwa Ibom State Polytechnic , Ikot Osurua Ikot Ekpene

Abstract— **In this program, the design of satellite orbital Two Line Element (TLE) to Cartesian Position Vector (CVC) coordinates (X,Y,Z) transformation program is presented. The TLE dataset consists of eccentricity which is denoted as e; inclination angle with unit in degrees and denoted i, right ascension of the ascending node with unit in degrees and denoted Ω, mean anomaly with unit in degrees and denoted as M, argument of the perigee with unit in degrees and denoted as ω, mean motion with unit in revolutions per day and denoted as n, and revolution number at epoch and denoted as N_{ap}. The program designed consisted of three modules and the detailed algorithm for each of the modules is presented. Five cases study satellites were used in the study and the output data includes the orbital period, the semi major axis, the semi minor axis, the eccentric anomaly, and the Cartesian coordinates X, Y, and Z for the five case study satellites. The results for the five satellites were presented in tables and graphs. The results showed that for the five satellites, the correlation between E and M is 0.984041669 whereas the correlation between E and e is 0.563807015. In essence E is more correlated to M than it is to e. In all, the results showed that the absolute value of X,Y,Z coordinates can be as high as the semi major axis of the satellite's orbit.**

Keywords — Coordinates Transformation, Two Line Element , Orbital Coordinates, Satellite, Cartesian Position Vector Coordinates

1. Introduction

Satellites position in orbits are in different ways or formats known as coordinate systems [1,2,3,4,5,6,7,8,9,10,11,12,13]. Each of the coordinate systems presents the location of the satellite in a way that is useful for some specific applications or they make it easier or better to visualize and apply the coordinates in specific analysis and processes. One of the most popular ways of representing satellites orbital parameters is the Two Line Element (TLE) format [14,15, 16,17, 18,19, 20,21,22,23]. The TLE is used to capture and store historical data about the positions of the satellite at any given instance of time, referred to as epoch. However, the TLE format is not suitable for certain applications of the satellites data [24,25, 26,27, 28,29, 30,31, 32]. As such, coordinate transformation is needed [33,34, 35,36, 37,38, 39].

Accordingly, a program is designed in this paper for the transformation of satellites TLE datasets to their corresponding Cartesian position vector coordinates [40,411,42,43,44,45,46]. The program algorithms are presented along with the numerical computation results obtained from the program for a selected number of case study satellites. The program is implemented using the Visual Basic for Application [47,48,49,50,51,52].

2. Methodology

The program design presented in this paper can read in a satellite's Two Line Element (TLE) dataset and then compute the equivalent Cartesian Position Vector (CPV) format transformation of the TLE dataset.

The TLE dataset consists of eccentricity which is denoted as e; inclination angle with unit in degrees and denoted i, right ascension of the ascending node with unit in degrees and denoted Ω, mean anomaly with unit in degrees and denoted as M, argument of the perigee with unit in degrees and denoted as ω, mean motion with unit in revolutions per day and denoted as n, and revolution number at epoch and denoted as N_{ap}.

The satellite Cartesian coordinates, x, y and z are computed from the listed TLE dataset , namely, e, i, Ω, M, ω, n, and N_{ap}. However, some other orbital parameters of the satellite that are required for the computation of the Cartesian coordinates, x, y and z are determined from the given TLE dataset. Such additional orbital parameters include; the orbital period with unit as days and denoted as T, the semi major axis, with unit as km and denoted as a, the semi minor axis with unit as km and denoted b and the eccentricity anomaly with unit in degrees is denoted E. This set of additional orbital parameters are denoted in this paper as secondary orbital elements, namely, T, a, b, and E. The computation of T, a and b are based on simple closed-form analytical expressions. However, the computation of E from the values of M and e is performed using iterative procedure presented by [53]. The analytical expressions for the computation of the satellite Cartesian coordinates, x, y and z are given as follows;

$$\mathbf{T} = \frac{1}{n} \quad (1)$$

$\mathrm{GM} = 2.9755364\mathrm{x}10^{15} km^3/day^2$.

$$\mathbf{a} = \sqrt[3]{\left(\left(\frac{\mathrm{GM}}{4\pi^2}\right)T^2\right)} \quad (2)$$

$$\mathbf{b} = \sqrt[2]{\mathbf{a}^2(\mathbf{1}-\mathbf{e}^2)} \quad (3)$$

$$\mathbf{E} = \mathbf{M} + \mathbf{e}(\sin(\boldsymbol{E})) \quad (4)$$

E is determined using iterative method based on the algorithm presented by [53];

$$\mathbf{x3} = (\mathbf{a})\cos(\boldsymbol{E}) - (\mathbf{a})\boldsymbol{e} \quad (5)$$

$$\boldsymbol{y3} = (\mathbf{b})\sin(\boldsymbol{E}) \quad (6)$$

$$\boldsymbol{z3} = \mathbf{0} \quad (7)$$

$$\boldsymbol{x2} = (\boldsymbol{x3})\cos(\boldsymbol{\omega}) - (\boldsymbol{y3})\sin(\boldsymbol{\omega}) \quad (8)$$

$$\boldsymbol{y2} = (\boldsymbol{x3})\sin(\boldsymbol{\omega}) + (\boldsymbol{y3})\cos(\boldsymbol{\omega}) \quad (9)$$

$$\boldsymbol{z2} = \boldsymbol{z3} \quad (10)$$

$$\boldsymbol{x1} = \boldsymbol{x2} \quad (11)$$

$$\boldsymbol{y1} = (\boldsymbol{y2})\cos(\boldsymbol{i}) - (\boldsymbol{z2})\sin(\boldsymbol{i}) \quad (12)$$

$$\boldsymbol{z1} = (\boldsymbol{y2})\sin(\boldsymbol{i}) + (\boldsymbol{z2})\cos(\boldsymbol{i}) \quad (13)$$

$$\boldsymbol{x} = (\boldsymbol{x1})\cos(\Omega) - (\boldsymbol{y1})\sin(\Omega) \quad (14)$$

$$\mathbf{y} = (\boldsymbol{x1})\sin(\Omega) + (\mathbf{y1})\cos(\Omega) \quad (15)$$

$$\boldsymbol{z} = \boldsymbol{z1} \quad (16)$$

The three modules designed for the computation of the satellite Cartesian coordinates, x, y and z from the TLE dataset are as follows;

i. Algorithm 1 Module1 Input TLE_Compute_XYZ()
ii. **Algorithm 2** Module 2 Compute_E(M, e)
iii. Algorithm 3 Module 3 Compute_XYZ (e, i, **Ω**, M, **ω**, n, $\boldsymbol{N_{ap}}$, T, a, b, E, x, y, z)

The detail algorithm for each of the three modules are presented next.

i). Algorithm 1 Module1 Input TLE_Compute_XYZ()

Algorithm 1 The procedure for Module1 Input TLE_Compute_XYZ()

1:Inpute Satellite_name, e, i, Ω, M, ω, n, N_{ap}
2: $\mathrm{T} = \frac{1}{n}$
3: $\mathrm{GM} = 2.9755364\mathrm{x}10^{15}$
4:$\mathrm{a} = \sqrt[3]{\left(\left(\frac{\mathrm{GM}}{4\pi^2}\right)T^2\right)}$
5:$\mathrm{b} = \sqrt[2]{\mathrm{a}^2(1-\mathrm{e}^2)}$
6: E =Module_Compute E(M,e) // call module compute E(M,e) and assign the returned value from the module to E
7: Call Module 3 ComputeXYZ (e, i, Ω, M, ω, n, N_{ap}, T, a, b, E, x, y, z)
8: Return E(k)
10: End Module compute E()

ii). **Algorithm 2** Module 2 Compute_E(M, e).

E is determined using iterative method based on the algorithm presented by [53] and it is presented as follows;

Algorithm 2 The procedure for Module 2 Compute_E(M, e)

1: Input er
2: k =0;
3: E(k) = M
4: fE(k) = E(k) – M – e*Sin(E(k))
5: dfE(k) = 1 – e*Cos (E(k))
6: k = k+1
7: E(k) = E(k-1) - $\frac{E(k-1)-M-e*Sin(E(k-1))}{1-e*Cos(E(k-1))}$
8: if ($|E(k)-E(k-1)| >$ |er|) then Goto step 4endif
9: Return E(k)
10: End Module compute E()

iii). **Algorithm 3 Module 3 Compute_XYZ** (Satellite_name, , e, i, **Ω, M, ω, n,** $\boldsymbol{N_{ap}}$**, T, a, b, E, x, y, z)**

Algorithm 3 The procedure for Module 3 Compute_XYZ (Satellite_name, e, i, **Ω**, M, **ω**, n, $\boldsymbol{N_{ap}}$, T, a, b, E, x, y, z)

1: $x3 = (\mathrm{a})\cos(E) - (\mathrm{a})e$
2: $y3 = (\mathrm{b})\sin(E)$
3: $z3 = 0$
4: $x2 = (x3)\cos(\omega) - (y3)\sin(\omega)$
5: $y2 = (x3)\sin(\omega) + (y3)\cos(\omega)$
6: $z2 = z3$
7: $x1 = x2$
8: $y1 = (y2)\cos(i) - (z2)\sin(i)$

$z1 = (y2)\sin(i) + (z2)\cos(i)$
$x = (x1)\cos(\Omega) - (y1)\sin(\Omega)$
$y = (x1)\sin(\Omega) + (y1)\cos(\Omega)$
$z = z1$
Output Satellite name , e, i, Ω, M, ω, n, N_{ap}
Output Satellite name, T, a, b, E, x, y, z
Return
End Module compute E()

3 Numerical Example

The two line element dataset for five selected satellites are used to demonstrate how the programs presents the results of the coordinate transformation. The five satellites, as presented in Table 1 includes RESURS-DK 1, CUBESAT XI-V and CALSPHERE 1 which are low Earth orbit (LEO) satellites, LAGEOS 1 which is a medium Earth orbit (MEO) satellite and INMARSAT 3-F1 which is a geostationary Earth orbit (MEO) satellite. All the five selected satellites are operational. The NORAD Two Line Element (TLE) dataset for the five active satellites, with data current as of 2022 Jul 02 12:05:26 UTC (Day 183) are presented in Figure 1 as accessed from [54].

Table 1 The five selected case study satellites (Source: https://in-the-sky.org/ and https://www.n2yo.com/)

S/N	NORAD ID	Satellite Name	Launch date	Status	Category	Orbital height (km)	Owner
1	29228	RESURS-DK 1	14 Jun 2006	Operational	Earth Resources (LEO)	556	Commonwealth of Independent States (former USSR)
2	28895	CUBESAT XI-V	26 Oct 2005	Operational	Amateur radio and CubeSats (LEO)	679	Japan
3	900	CALSPHERE 1	05 Oct 1964	Operational	Radar Calibration (LEO)	985	United States
4	8820	LAGEOS 1	03 May 1976	Operational	Geodetic (MEO)	5893	United States
5	23839	INMARSAT 3-F1	02 Apr 1996	Operational	Geostationary (GEO)	35866	International Mobile Satellite Organization (INMARSAT

```
RESURS-DK 1
1 29228U 06021A   22182.85702829 .00000388  00000-0  35839-4 0  9998
2 29228  69.9357  92.3092 0003328 355.7535   4.3598 15.03268924884546

CUBESAT XI-V
1 28895U 05043F   22182.79982544  .00000335  00000-0  72377-4 0  9998
2 28895  98.1087 313.9583 0018036  96.4060 263.9198 14.64366421889518
CALSPHERE 1
1 00900U 64063C   22183.60674226  .00000326  00000-0  33757-3 0  9996
2 00900  90.1742  41.1916 0026876 341.5197  71.8743 13.73830012872741

LAGEOS 1
1 08820U 76039A   22182.72361315  .00000013  00000-0  00000-0 0  9990
2 08820 109.8554  43.8842 0045063 251.7017 295.8809  6.38664942820764

INMARSAT 3-F1
1 23839U 96020A   22182.42771380 -.00000255  00000-0  00000-0 0  9992
2 23839   7.5677  58.0387 0009065  47.6313 261.1318  0.99987079 95783
```

Figure 1 The NORAD Two Line Element (TLE) dataset for the five active satellites, with data current as of 2022 Jul 02 12:05:26 UTC (Day 183) accessed from [54].

4. Results and Discussions

The detailed TLE dataset were extracted from the NORAD Two Line Element (TLE) dataset for the five active satellites presented in Figure 1 and the extracted TLE parameters are shown in Table 2. The datasets in Table 2 are then used to compute the orbital period, semi major axis, semi minor axis and the eccentric anomaly, as well as the Cartesian coordinates X, Y, and Z for the five case study satellites and the results are shown in Table 3. Furthermore, the graph of the eccentricity anomaly E versus mean anomaly (M) and the eccentricity anomaly (E) versus eccentricity (e) were plotted as shown in Figure 2 and Figure 3respectively. It was also determined that for the five satellites, the correlation between E and M is 0.984041669 whereas the correlation between E and e is 0.563807015. In essence E is more correlated to M. The bar chart of the Cartesian coordinates X, Y, and Z for the five case study satellites is given in Figure 4.

Table 2 The detail TLE dataset extracted for Figure 1 for the five selected satellites

	1	2	3	4	5	6	7
Satellite Name	**e**	**i (deg)**	**Ω (deg)**	**M (deg)**	**ω (deg)**	**n (rev/day)**	**Nap**
RESURS-DK 1	0.0003328	69.9357	92.3092	4.3598	355.754	15.03269	88454
CUBESAT XI-V	0.0018036	98.1087	313.958	263.92	96.406	14.64366	88951
CALSPHERE 1	0.0026876	90.1742	41.1916	71.8743	341.52	13.7383	87274
LAGEOS 1	0.0045063	109.855	43.8842	295.881	251.702	6.386649	82076
INMARSAT 3-F1	0.0009065	7.5677	58.0387	261.132	47.6313	0.999871	9578

Table 3 The results of the computation of the orbital period, semi major axis, semi minor axis, the eccentric anomaly, the Cartesian coordinates X, Y, and Z for the five case study satellites

0	8	9	10	11	12	13	14
Satellite Name	T (day)	a (km)	b (km)	E (deg)	X	Y	Z
RESURS-DK 1	0.0665217	6,934.96	6,934.96	4.36	-284.15	6,926.82	13.21
CUBESAT XI-V	0.0682889	7,057.25	7,057.24	263.82	4,898.12	-5,082.55	14.68
CALSPHERE 1	0.0727892	7,363.99	7,363.96	72.02	3,290.80	2,856.07	5,928.91
LAGEOS 1	0.1565766	12,271.18	12,271.06	295.65	-9,116.36	-8,052.97	-1,427.15
INMARSAT 3-F1	1.0001292	42,244.73	42,244.72	207.75	28,744.81	-30,531.89	-5,387.16

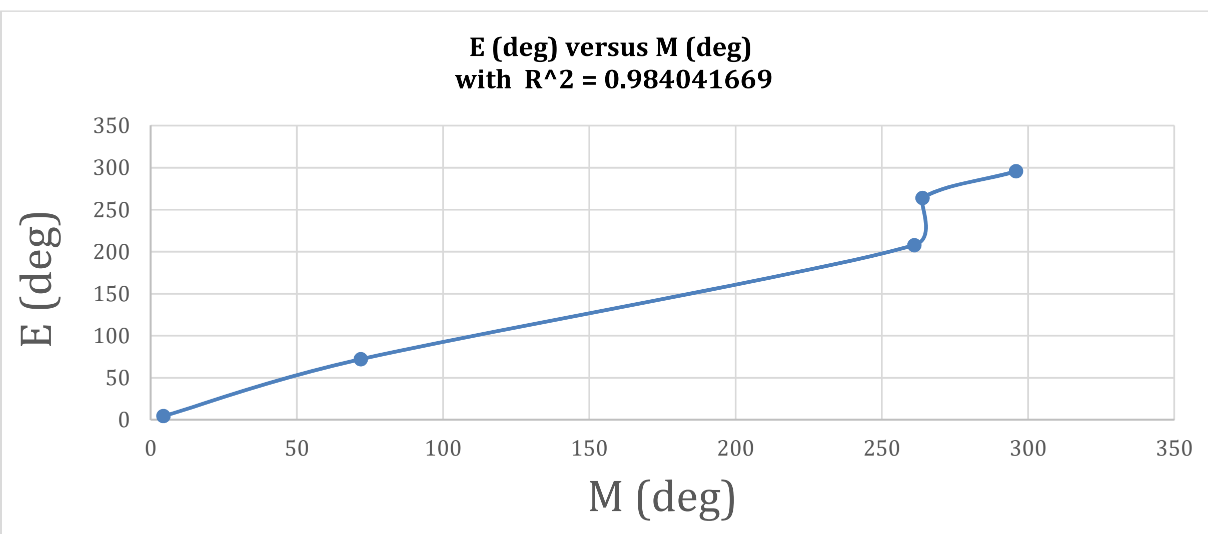

Figure 2 The graph of the eccentricity anomaly, E versus mean anomaly (M) for the five case study satellites

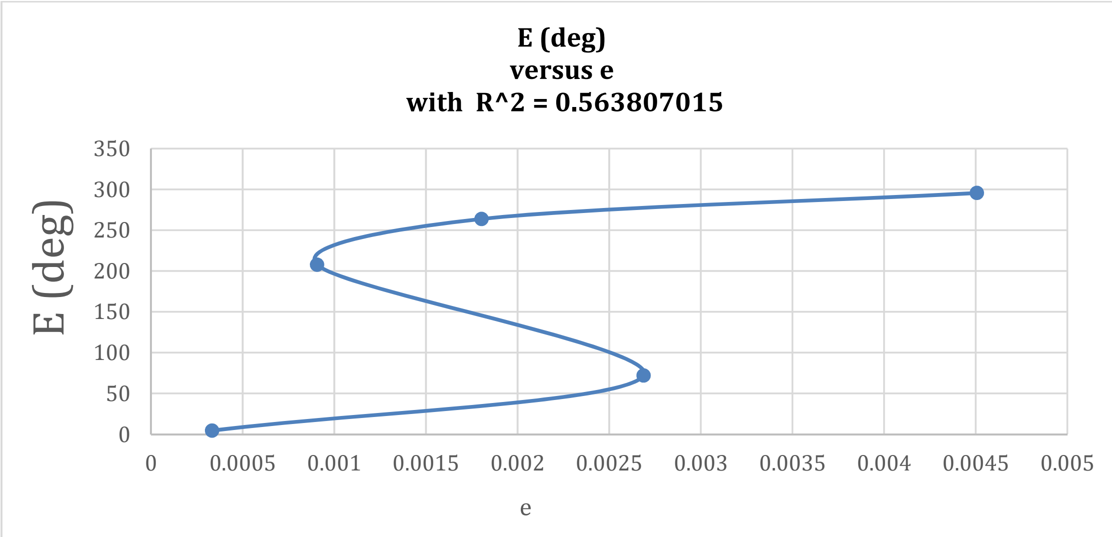

Figure 3 The graph of the eccentricity anomaly, E versus eccentricity (e) for the five case study satellites

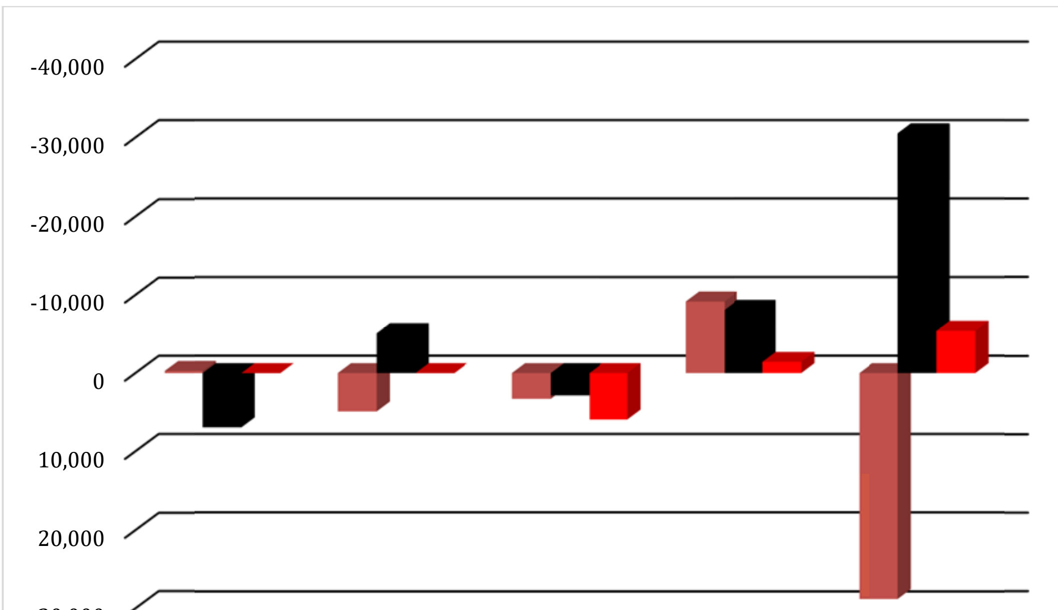

	RESURS-DK 1	CUBESAT XI-V	CALSPHERE 1	LAGEOS 1	INMARSAT 3-F1
X	-284.15	4,898.12	3,290.80	-9,116.36	28,744.81
Y	6,926.82	-5,082.55	2,856.07	-8,052.97	-30,531.89
Z	13.21	14.68	5,928.91	-1,427.15	-5,387.16

Figure 4 The bar chart of the Cartesian coordinates X, Y, and Z for the five case study satellites

5. Conclusion

The design of the modules and their corresponding algorithms for computing the Cartesian coordinates X, Y, and Z of a satellite from the two line element dataset are presented. The design consists of three modules and five case study satellites are used to show how the program modules are applied in the computation. In the numerical examples, the output data includes the orbital period, the semi major axis, the semi minor axis, the eccentric anomaly, and the Cartesian coordinates X, Y, and Z for the five case study satellites

References

1. Zhang, P., Xu, C., Hu, C., & Chen, Y. (2012). Coordinate transformations in satellite navigation systems. In *Advances in Electronic Engineering, Communication and Management Vol. 2* (pp. 249-257). Springer, Berlin, Heidelberg.

2. Maling, D. H. (2013). *Coordinate systems and map projections*. Elsevier.
3. Noureldin, A., Karamat, T. B., & Georgy, J. (2013). Fundamentals of inertial navigation, satellite-based positioning and their integration.
4. Ihde, J., Sánchez, L., Barzaghi, R., Drewes, H., Foerste, C., Gruber, T., ... & Sideris, M. (2017). Definition and proposed realization of the International Height Reference System (IHRS). *Surveys in geophysics*, *38*(3), 549-570.
5. Lu, Z., Qu, Y., & Qiao, S. (2014). *Geodesy*. Springer: Berlin/Heidelberg, Germany.
6. Kovalevsky, J., Mueller, I. I., & Kolaczek, B. (Eds.). (2012). *Reference frames: in astronomy and geophysics* (Vol. 154). Springer Science & Business Media.
7. Wolf, P. R., Dewitt, B. A., & Wilkinson, B. E. (2014). *Elements of Photogrammetry with Applications in GIS*. McGraw-Hill Education.
8. Lutz, E., Werner, M., & Jahn, A. (2012). *Satellite systems for personal and broadband communications*. Springer Science & Business Media.
9. Soler, T., & Hothem, L. D. (1988). Coordinate systems used in geodesy: Basic definitions and concepts. *Journal of surveying engineering*, *114*(2), 84-97.
10. Guo, J., Wang, Y., Shen, Y., Liu, X., Sun, Y., & Kong, Q. (2018). Estimation of SLR station coordinates by means of SLR measurements to kinematic orbit of LEO satellites. *Earth, Planets and Space*, *70*(1), 1-11.
11. Aleksandrov, A. Y., & Tikhonov, A. A. (2013). Monoaxial electrodynamic stabilization of Earth satellite in the orbital coordinate system. *Automation and Remote Control*, *74*(8), 1249-1256.
12. Zebker, H. A. (2017). User-friendly InSAR data products: Fast and simple timeseries processing. *IEEE Geoscience and Remote Sensing Letters*, *14*(11), 2122-2126.
13. Montenbruck, O., Schmid, R., Mercier, F., Steigenberger, P., Noll, C., Fatkulin, R., ... & Ganeshan, A. S. (2015). GNSS satellite geometry and attitude models. *Advances in Space Research*, *56*(6), 1015-1029.
14. Lambeck, K. (1973). Precession, nutation and the choice of reference system for close earth satellite orbits. *Celestial mechanics*, *7*(2), 139-155.
15. Vallado, D. A., & Cefola, P. J. (2012, October). Two-line element sets-Practice and use. In *63rd International Astronautical Congress, Naples, Italy* (pp. 1-14).
16. Croitoru, E. I., & Oancea, G. (2016). Satellite tracking using norad two-line element set format. *Scientific Research and Education in the Air Force-AFASES*, *1*, 423-431.
17. Maiti, A., Majumdar, S., Shukla, S., Koti, S. R., & Gupta, P. K. (2018). An open source web-gis based precise satellite tracking and visualisation tool using two line element data. *ISPRS Annals of the Photogrammetry, Remote Sensing and Spatial Information Sciences*, *4*, 109-114.
18. Früh, C., & Schildknecht, T. (2012). Accuracy of two-line-element data for geostationary and high-eccentricity orbits. *Journal of guidance, control, and dynamics*, *35*(5), 1483-1491.
19. Yim, H. J., & Chung, D. W. (2012). Validation on residual variation and covariance matrix of USSTRATCOM Two Line Element. *Journal of Astronomy and Space Sciences*, *29*(3), 287-293.
20. Bai, X., Liao, C., Pan, X., & Xu, M. (2019). Mining two-line element data to detect orbital maneuver for satellite. *IEEE Access*, *7*, 129537-129550.
21. Kahr, E., Montenbruck, O., & O'Keefe, K. P. (2013). Estimation and analysis of two-line elements for small satellites. *Journal of Spacecraft and Rockets*, *50*(2), 433-439.
22. Lidtke, A. A., Gondelach, D. J., & Armellin, R. (2019). Optimising filtering of two-line element sets to increase re-entry prediction accuracy for GTO objects. *Advances in Space Research*, *63*(3), 1289-1317.
23. Nugroho, M., & Khamsah, N. M. N. (2018, September). Study on Impact of Outdated Two-Line Element Sets in Tracking of LAPAN-A2 and LAPAN-A3 Satellites. In *2018 IEEE International Conference on Aerospace Electronics and Remote Sensing Technology (ICARES)* (pp. 1-6). IEEE.
24. Speretta, S., Sundaramoorthy, P., & Gill, E. (2017, April). Long-term performance analysis of NORAD Two-Line Elements for CubeSats and PocketQubes. In *11th IAA Symposium on Small Satellites for Earth Observation* (pp. 1-6). DLR.
25. Shi, C., Li, W., Li, M., Zhao, Q., & Sang, J. (2015). Calibrating the scale of the NRLMSISE00 model during solar maximum using the two line elements dataset. *Advances in Space Research*, *56*(1), 1-9.
26. Elhag, M. A., Yassin, A. A., Babiker, M. E., & Abd Elmageed, E. A. E. (2013, August). The unscented Kalman filter applied to satellite orbit determination using only publically available two-line element sets. In *2013 INTERNATIONAL CONFERENCE ON COMPUTING, ELECTRICAL AND ELECTRONIC ENGINEERING (ICCEEE)* (pp. 464-469). IEEE.
27. Riesing, K. (2015). Two line element sets of cubesats in leo: Accuracy assessment and estimation techniques for improvement. In *29th Annual AIAA/USU Conference on Small Satellites*.
28. Flohrer, T., Krag, H., & Klinkrad, H. (2008). Assessment and categorization of TLE orbit errors for the US SSN catalogue. *risk*, *8*(9), 10-11.
29. Vallado, D. A., & Cefola, P. J. (2012, October). Two-line element sets-Practice and use. In *63rd*

International Astronautical Congress, Naples, Italy (pp. 1-14).
30. Paulet, T., & Cazabonne, B. (2021). An open-source solution for TLE based Orbit Determination. In *8th European conference on space debris*.
31. Ly, D., Lucken, R., & Giolito, D. (2020). Correcting TLEs at epoch: Application to the GPS constellation. *Journal of Space Safety Engineering*, *7*(3), 302-306.
32. Weiping, L., Hongxing, Q., & Qi, D. (2012, June). Iterative method for two line element conversion. In *2012 IEEE International Conference on Information and Automation* (pp. 811-813). IEEE.
33. Montenbruck, O., Gill, E., & Lutze, F. (2002). Satellite orbits: models, methods, and applications. *Appl. Mech. Rev.*, *55*(2), B27-B28.
34. Bouman, J., Ebbing, J., & Fuchs, M. (2013). Reference frame transformation of satellite gravity gradients and topographic mass reduction. *Journal of Geophysical Research: Solid Earth*, *118*(2), 759-774.
35. Mok, E. (1992). A model for the transformation between satellite and terrestrial networks in Hong Kong. *Survey Review*, *31*(244), 344-350.
36. Noureldin, A., Karamat, T. B., & Georgy, J. (2013). Fundamentals of inertial navigation, satellite-based positioning and their integration.
37. Deprit, A., & Rom, A. (1970). The main problem of artificial satellite theory for small and moderate eccentricities. *Celestial mechanics*, *2*(2), 166-206.
38. Seeber, G. (2008). Satellite geodesy. In *Satellite Geodesy*. de Gruyter.
39. Frey, S., & Colombo, C. (2021). Transformation of satellite breakup distribution for probabilistic orbital collision hazard analysis. *Journal of Guidance, Control, and Dynamics*, *44*(1), 88-105.
40. Stoll, E., Letschnik, J., & Kebschull, C. (2020). II-3: Ground-based Satellite Tracking. *Nanosatellites: Space and Ground Technologies, Operations and Economics*, 471-494.
41. Riesing, K. (2015). Orbit determination from two line element sets of ISS-deployed cubesats.
42. Popescu, G. (2014). Pixel geolocation algorithm for satellite scanner data. *Scientific Papers. Series E. Land Reclamation, Earth Observation & Surveying, Environmental Engineering*, *3*, 127-136.
43. Szabova, M., & Duchon, F. (2016). Survey of GNSS coordinates systems. *European Scientific Journal*, *12*(24).
44. Shi, Q. Q., Tian, A. M., Bai, S. C., Hasegawa, H., Degeling, A. W., Pu, Z. Y., ... & Liu, Z. Q. (2019). Dimensionality, coordinate system and reference frame for analysis of in-situ space plasma and field data. *Space Science Reviews*, *215*(4), 1-54.
45. Sinclair, A. J., Sherrill, R. E., & Lovell, T. A. (2015). Use of Cartesian-coordinate calibration for satellite relative-motion control. *Journal of Guidance, Control, and Dynamics*, *38*(9), 1842-1847.
46. Hallaj, M. A. A., & Assadian, N. (2015). Tethered satellite system control using electromagnetic forces and reaction wheels. *Acta Astronautica*, *117*, 390-401.
47. Осетрова, И. С., & Осипов, Н. А. (2013). Microsoft Visual Basic for Application.
48. Rohaeti, E. E., Bernard, M., & Primandhika, R. B. (2019). Developing interactive learning media for school level mathematics through open-ended approach aided by visual basic application for excel. *Journal on Mathematics Education*, *10*(1), 59-68.
49. Yan, W., & Hongliang, H. (2012). Hydropower Computation Using Visual Basic for Application Programming. *Physics Procedia*, *24*, 37-43.
50. Rohaeti, E. E., Bernard, M., & Novtiar, C. (2019). Pengembangan media visual basic application untuk meningkatkan kemampuan penalaran siswa SMP dengan pendekatan open-ended. *SJME (Supremum Journal of Mathematics Education)*, *3*(2), 95-107.
51. Del Sole, A. (2015). *Visual Basic 2015 Unleashed*. Sams Publishing.
52. Ngo-Ye, T. L. (2015). Microsoft Visual Basic For Application (VBA)/Macro. In *Alabama State University. Conference Paper: The Eighteent Annual Conference of the Southers Association for Information System (SAIS 2015). At Hilton Head Island, South California*.
53. Simeon, O. (2014) Comparative Evaluation Of Initial Value Options For Numerical Iterative Solution To Eccentric Anomalies In Kepler's Equation For Orbital Motion. Journal of Multidisciplinary Engineering Science and Technology (JMEST) Vol. 1 Issue 5, December – 2014
54. NORAD GP Element Sets showing current data for active satellites, with data current as of 2022 Jul 02 12:05:26 UTC (Day 183). Available at https://celestrak.org/NORAD/elements/gp.php?GROUP=active&FORMAT=tle